Check for
updates

Economical Approach for Determination of Kojic Acid by Nanostructured Ionic Liquid-Based Carbon Paste Sensor

Sanaz Avazpour[1] · Abbas Pardakhty[2] · Ebrahim Nabatian[3] · Saeid Ahmadzadeh[2,4]

Abstract

An economical and sensitive nanostructured sensor based on carbon paste electrode (CPE) for the determination of kojic acid (KA) was developed in the current work. The applied CPE was modified with 1-butyl-3-methylimidazolium tetrafluoroborate (1B3MITFB) as a conductive binder and NiO nanoparticles (NiO/NPs). The proposed modified ionic liquid-based carbon paste electrode showed satisfactory concentration range and lower detection limit of 5.0–600 μM and 0.8 μM at phosphate buffer pH 6.0, respectively. An acceptable reproducibility with a satisfactory analytical characteristic was observed for the proposed sensor in the presence of common interfering compounds. The observed irreversible oxidation behavior of KA at the surface of the NiO/NPs/1B3MITFB/MCPE was controlled under the diffusion step and the diffusion coefficient (D) at the mass transport limited rate found to be 2.3×10^{-4} cm^2 s^{-1}. According to the slope of the Tafel plot, the value of 0.625 was calculated for the electron transfer coefficient (α). The acquired data from electrochemical impedance spectroscopy studies confirmed that the presence of NiO NPS and 1B3MITFB as a conductive binder resulted in a significant increase in the electro-oxidation signal of KA. The value of 12.3 kΩ for the R_{ct} of unmodified CPE decreased to the value of 1.7 kΩ for the modified electrode. The obtained results revealed that the proposed modified ionic liquid-based carbon paste electrode could be applied successfully for the analysis of trace amounts of KA in biological samples such as blood serum, urine, and pharmaceutical samples such as liposome carriers containing KA as well as food samples such as vinegar. The synthesized NiO nanoparticles were characterized using XRD and EDAX analyses. The morphology of NiO/NPs is further characterized by SEM.

Keywords Kojic acid analysis · Nanostructured sensor · Voltammetry · NiO nanoparticle · Pharmaceutical sample

1 Introduction

Kojic acid (KA) is extensively used in pharmaceutical products to obtain a skin-lightening effect in personal care products since it prevents melanin formation. Moreover, due to the functional role of KA as an enzyme inhibitor in the biosynthesis of dihydroxyphenylalanine, it applied as a preservative agent to avoid microbial and chemical degradation of food [1, 2].

On the other hand, the presence of 4-pyrone in the KA structure may cause a carcinogenic effect that threatens human health [3]. However, some researcher believes that animal experiments such as rat data cannot generalize to human beings and the usual level of KA in foods would not cause harmful effect on human health [1]. Nevertheless, due to the unfavorable effect of KA at relatively higher concentrations, especially in foods and cosmetics stuff, it is of great importance to consider with high sensitivity about the safety and quality control of the mentioned products. Therefore, developing an economical and fast analytical approach for the quantitative evaluation of the trace level of KA is considered desirable.

Various techniques developed for quantitative determination KA such as ion-pair liquid chromatography (IPLC) [4], high-performance liquid chromatography (HPLC) [5], fluorescent detection [6], and electrochemical method [7]. Among the mentioned techniques, electrochemical methods

✉ Saeid Ahmadzadeh
saeid.ahmadzadeh@kmu.ac.ir; chem_ahmadzadeh@yahoo.com

1 Student Research Committee, Kerman University of Medical Sciences, Kerman, Iran

2 Pharmaceutics Research Center, Institute of Neuropharmacology, Kerman University of Medical Sciences, Kerman, Iran

3 Department of Chemistry, Faculty of Sciences, Shahid Bahonar University of Kerman, Kerman, Iran

4 Pharmaceutical Sciences and Cosmetic Products Research Center, Kerman University of Medical Sciences, Kerman, Iran

such as voltammetry received attention due to offering opportunities such as sensitive and fast detection procedures and portability for the determination of electroactive compounds such as KA [8]. Due to the advantages such as lowering cost, easy, and fast preparation by providing a reproducible surface with a low residual current in electrochemical studies, ionic liquid-based carbon paste electrodes received growing attention recently.

Lately, nanostructured materials by unique chemical and electrical properties received extraordinary attention for developing the electrochemical sensors employed in the analysis of pharmaceutical and biological samples [9–12]. Due to the high surface area and great catalytic activity of metal-based nanoparticles with biocompatible properties, they employed to increase the current density of the electrochemical setup of biosensors in biological and food compound analysis. Moreover, to fabricate a sensitive electrochemical modified sensor, it is recommended to optimize the binder of the fabricated paste with a new generation of stable room temperature ionic liquids with high conductivity and broad electrochemical windows [13].

In the current work, we aimed to fabricate a high sensitive nanostructured sensor based on ionic liquid carbon pastes modified with NiO nanoparticles to investigate the electrooxidation of KA. The analytical performance of the proposed sensor was assessed by quantitative evaluation of KA in various real samples.

2 Material and Methods

2.1 Chemicals

Analytical grade kojic acid (KA), nickel (II) nitrate hexahydrate (Ni $(NO_3)_2 \cdot 6H_2O$), sodium hydroxide (NaOH), phosphoric acid (H_3PO_4), calcium sulfate ($CaSO_4$), magnesium nitrate hexahydrate ($Mg(NO_3)_2 \cdot 6H_2O$), potassium carbonate (K_2CO_3), sodium bicarbonate ($NaHCO_3$), 1-butyl-3-methylimidazolium tetrafluoroborate (1B3MITFB), graphite fine powder, and paraffin obtained from Sigma-Aldrich. Glucose, ascorbic acid, phenylalanine, methionine, histidine, cysteine, lysine, glycine, urea, and thiourea were obtained from Merck. Phosphate buffer solutions (PBS) with the desired pH values were prepared using 0.1 M H_3PO_4 and 0.1 M NaOH solutions.

2.2 Apparatus

The electrochemical investigations was carried out by a conventional three-electrode system including NiO/NPs/ 1B3MITFB/MCPE, platinum wire, and Ag/AgCl (3 M KCl) as working, counter, and the reference electrode, respectively, connected to Sama 500 potentiostat/galvanostat.

Electrochemical impedance spectroscopy (EIS) studies were carried out by Autolab PGSTAT204-Metrohm potentiostat/ galvanostat equipped with the FRA module. All experiments were carried out at room temperature. The pH adjustment was performed by a Metrohm pH meter model 827 pH lab. To evaluate the morphological aspects of the synthesized NiO nanoparticle, scanning electron microscopy (SEM) and X-ray diffraction analysis were carried out using VEGA3 XMU SEM and STOE diffractometer with Cu-Kα radiation ($k = 1.54$ Å), respectively,

2.3 Optimization the Modified Ionic Liquid-Based Carbon Paste Electrode

NiO/NPs/1B3MITFB/MCPE were prepared by mixing the appropriate amount of 1B3MITFB, paraffin oil, NiO/NPs, and graphite powder which mixed well in mortar for 3 h until a homogeneously moisten paste is achieved. The electrooxidation response of 500 µM KA was employed for optimization of the ratio of NiO/NPs to 1B3MITFB in the composition of modified ionic liquid-based carbon paste. The obtained result exhibited that the presence of 5.0% w/w of NiO/NPs and 10.0% w/w of 1B3MITFB in the proposed paste provide the highest oxidation peak current for a constant amount of KA. Hence, this composition is used for further studies.

## 3 Results and Discussion

3.1 NiO/NPs Characterization

XRD analyses were employed to analyze the synthesized NiO/NPs. The definite line broadening obtained from the XRD pattern revealed that the NPs synthesized successfully where the average diameter of synthesized NiO/NPs found to be about 20.8 nm using the Scherrer equation [14, 15]. The XRD patterns of NiO nanoparticle that is presented in Fig. 1a, revealing the reflection planes of (111), (200), (220), (311), and (222), correspond to the FCC structure of NiO nanoparticle according to JCPDS data. On the other hand, the elemental analysis of the synthesized nanoparticle was confirmed by the EDAX spectrum. The existence of nickel and oxygen elements confirmed that NiO/NPs synthesized successfully (see Fig. 1b).

Moreover, the SEM technique was employed to characterize the morphology of the synthesized NiO/NPs that is seen in Fig. 2; the observed dark points in nanoscale size correspond to the NiO/NPs.

3.2 Electrochemical Impedance Spectroscopy

EIS technique as an informative electrochemical approach employed in the current work to study the conductivity and

Fig. 1 a The XRD patterns of as-synthesized NiO nanoparticles. b The EDAX analysis of NiO nanoparticles
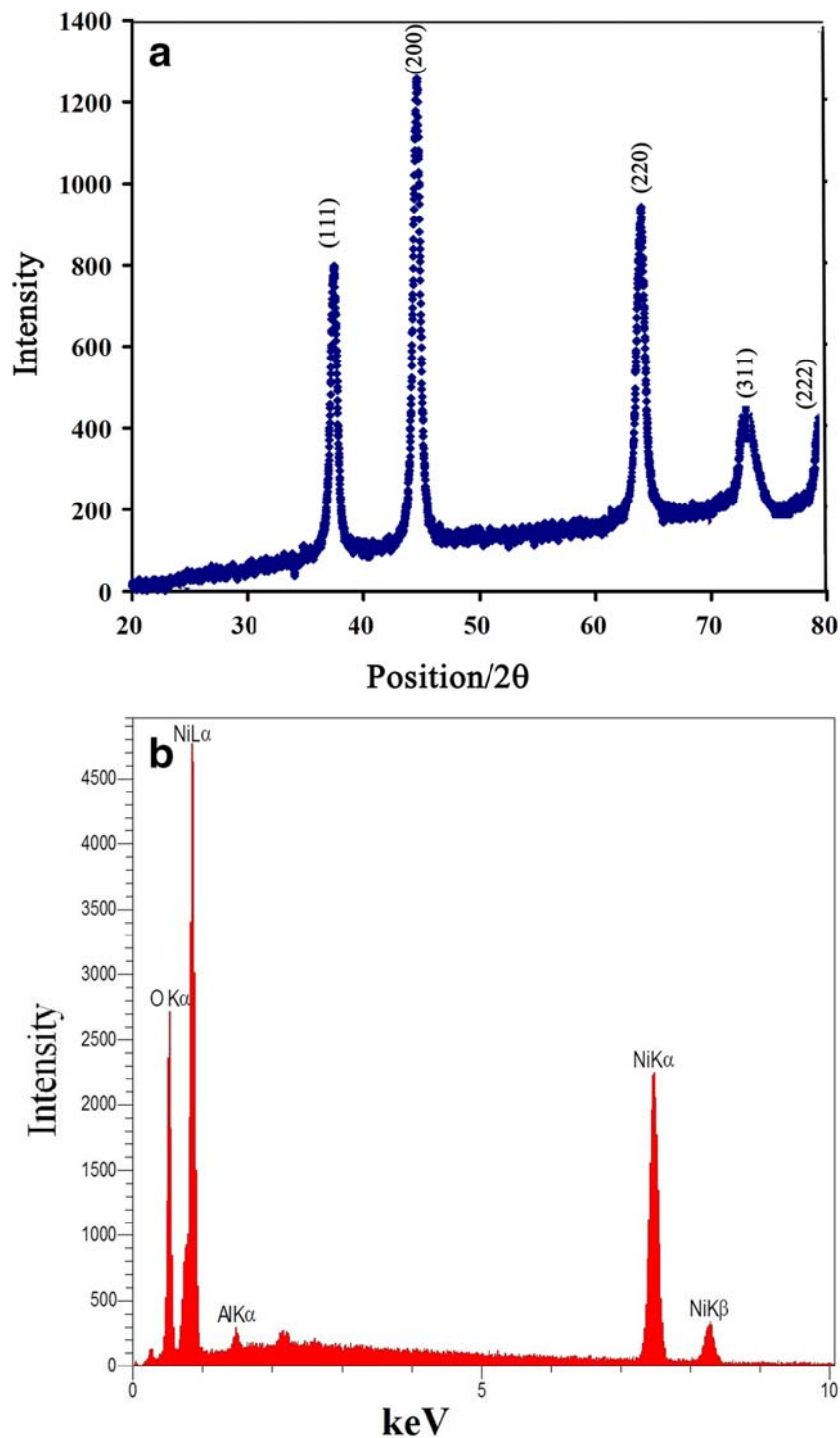
electron transfer kinetics of the surface of bare and modified electrodes throughout the step by step modification process. All researches carried out in 0.1 M PBS solution with frequencies ranging from 0.1 to 100 kHz. As seen from Fig. 3, the obtained Nyquist diagrams revealed an increase in the electrical conductivity of the prepared pastes from unmodified CPE (curve a) to the fully modified CPE namely NiO/NPs/ 1B3MITFB/MCPE (curve d) in the presence of 1.0 mM $[Fe(CN)_6]^{3-/4-}$ as a probe in EIS investigation.

The obtained data confirmed that the presence of NiO nanoparticles and 1B3MITFB as a conductive binder resulted in increasing the electro-oxidation signal of KA. The value of R_{ct} for unmodified CPE found to be 12.3 kΩ which is the highest value of R_{ct} in comparison with the other fabricated
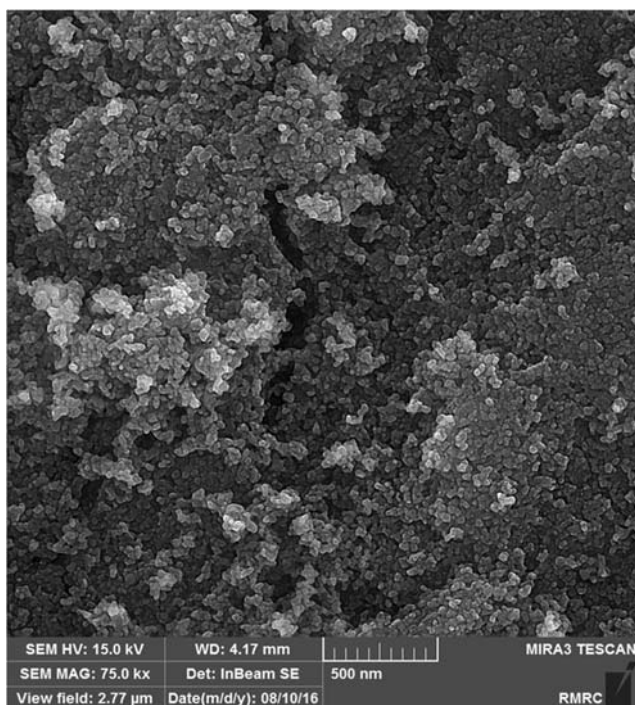
Fig. 2 The SEM image of NiO nanoparticles

modified CPEs in the current work because of paraffin usage as a non-conductive binder in its composition.

By adding NiO/NPs into the CPE to get the NiO/NPs/MCPE, the amount of R_{ct} lowered to 6.5 kΩ due to the presence of conductive NiO/NPs with high catalytic activity in NiO/NPs/MCPE composition. Alternatively, by addition of 1B3MITFB as a conductive binder into the CPE to get the 1B3MITFB/MCPE, the amount of R_{ct} was lowered to 3.1 kΩ. In contrast, using both NiO/NPs and 1B3MITFB in the composition of NiO/NPs/1B3MITFB/MCPE resulted in a maximum decreasing of R_{ct} value to the amount of 1.7 kΩ which

indicated that they performed as an efficient pathway for electron transfer between the proposed electrode and electrolyte. It is noteworthy to mention that the ratio of decrease in R_{ct} using EIS is in satisfactory agreement by the ratio of increase in oxidation current using cyclic voltammetry. The observed shape of Nyquist diagrams including a compressed semicircle portion and a straight line corresponds to the electron transfer resistance at the electrode surface and the diffusion-limiting step of the electrochemical process, respectively.

3.3 Voltammetric Investigation

The cyclic voltammetry method was employed to investigate the electro-oxidation of KA and the obtained electrochemical response in the presence of 500 μM KA on the surface of the bare and modified CPEs was demonstrated in Fig. 4 using phosphate buffer solution of 0.1 M (pH 6.0) at a scan rate of 100 mV s^{-1}. Curve (a) corresponding to NiO/NPs/1B3MITFB/MCPE revealed the maximum oxidation peak current of 118.6 μA with a substantial negative shift of the oxidation potential to 905 mV which confirmed the catalytic ability of the proposed electrode for KA electro-oxidation. As seen from curve (c) and (d), the contribution of NiO nanoparticles with superior electrical conductivity and large surface area in the composition of the bare electrode led to improving the peak current from 35.3 to 58.7 μA and reducing the KA oxidation potential from 1015 to 985 mV.

Moreover, curve (b) which corresponds to the presence of 1B3MITFB as a conductive binder in the composition of the bare revealed satisfactory enhancement in oxidation current to the value of 88.5 μA along with decreasing the overpotential of KA electro-oxidation to 935 mV. Due to the absence of a corresponding reduction peak for KA by scanning the

Fig. 3 Nyquist plots of CPE (**a**), NiO/NPs/MCPE (**b**), 1B3MITFB/MCPE (**c**), and NiO/NPs/1B3MITFB/MCPE (**d**) in the presence of 1.0 mM [Fe(CN)$_6$]$^{3-/4-}$ and 0.1 mol L^{-1} KCl. Conditions: pH, 6.0; E_{dc}, + 0.38 V vs. Ag/AgCl; E_{ac}, 5 mV; frequency range, 0.1 to 100,000 Hz. Inset: equivalent circuit for the system
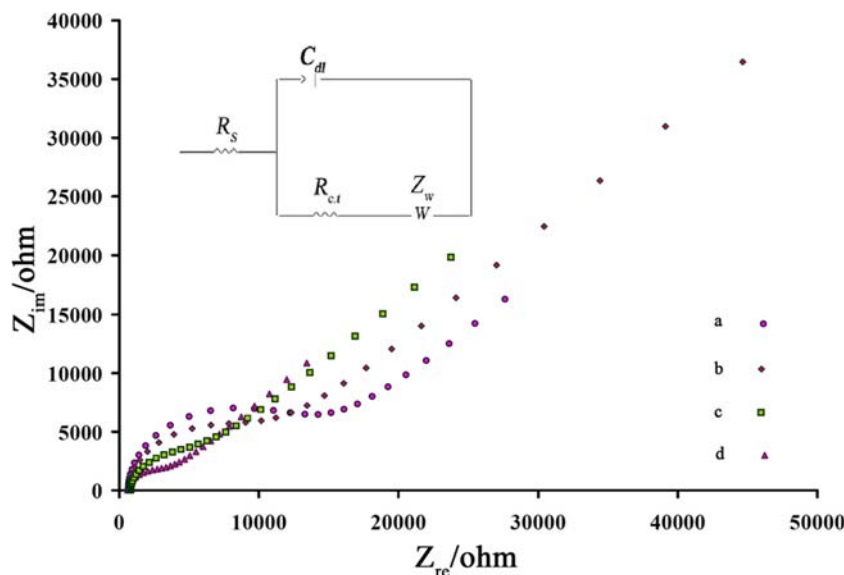
Fig. 4 Cyclic voltammograms of **a** NiO/NPs/1B3MITFB/MCPE, **b** 1B3MITFB/MCPE, **c** NiO/NPs/MCPE, and **d** CPE in the presence of 500 μM KA at pH 6.0, respectively
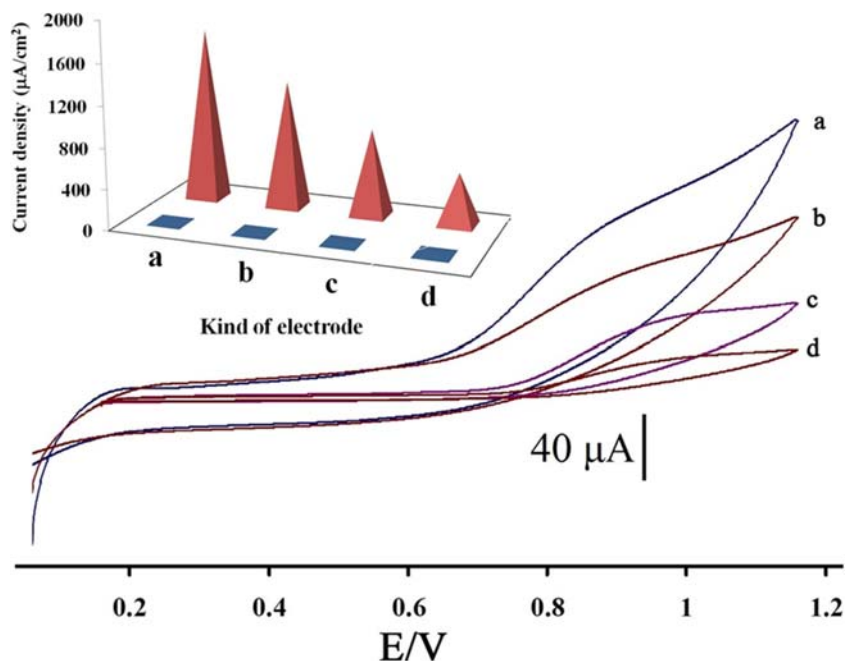
potential to the negative values, it concluded that electro-oxidation of KA was an irreversible reaction.
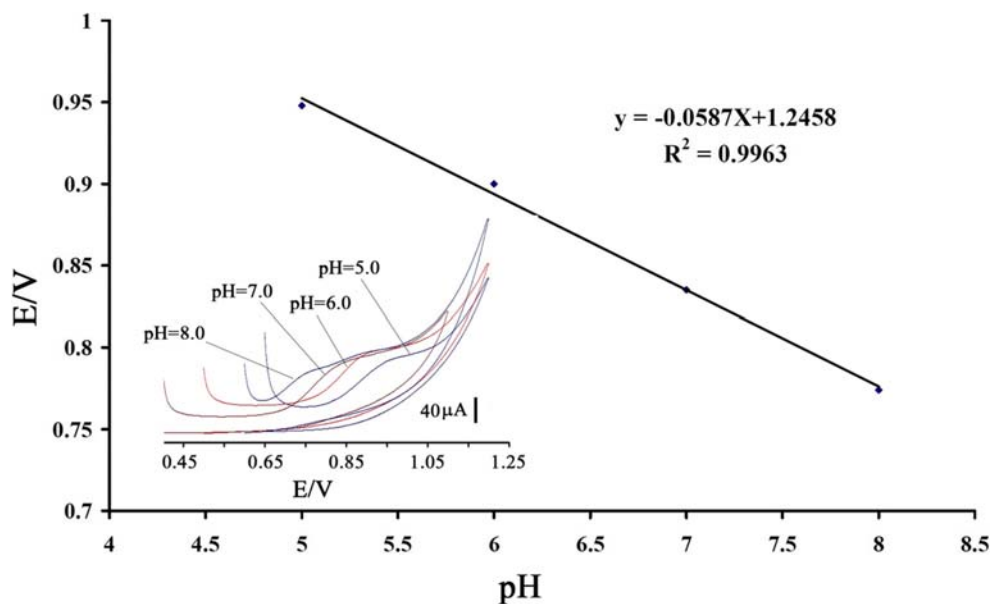
The current density at the surface of the proposed electrodes was calculated and demonstrated in Fig. 4 (inset) which confirmed the useful effect of NiO/NPs and 1B3MITFB presence by improving the active surface of the proposed modified CPE and led to the higher electrocatalytic activity at the surface of the prepared NiO/NPs/1B3MITFB/MCPE.
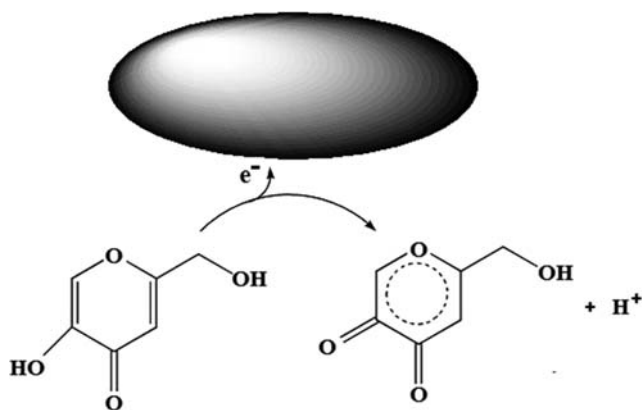
The literature survey revealed that due to the presence of the hydroxyl group in the KA structure, the pH of the electrolyte solution significantly affected the electro-oxidation of KA [1, 16, 17]. Therefore, NiO/NPs/1B3MITFB/MCPE was

employed to investigate the effect of pH on the electrochemical oxidation signal of KA. The obtained results indicated that the oxidation potentials (E_{pa}) of KA lowered to negative values as the solution pH increased varying from 5.0 to 8.0 (see Fig. 5 inset). The observed behavior attributed to the direct involvement of protons in the electro-oxidation process of KA.

As seen, the value of oxidation current improved from pH 5.0 to 6.0 and then diminished gradually by increasing the pH value from 6.0 to 8.0. Hence, the phosphate buffer solution with a pH of 6 taken as the proper medium and used throughout further experiments. As demonstrated in Fig. 5, the

Fig. 5 Plot of potential, E, vs. pH for the electro-oxidation of 500 μM KA at a surface of NiO/NPs/1B3MITFB/MCPE. Inset: influence of pH on cyclic voltammograms of KA at a surface of the modified electrode (pH 5–8, respectively) ($n = 1$)

$$y = -0.0587X + 1.2458$$
$$R^2 = 0.9963$$

Scheme 1 Electro-oxidation of kojic acid

NPs/1B3MITFB/MCPE was controlled under the diffusion step.

$$I_p = 8.488 \, \nu^{1/2} + 10.174 \; (r^2 = 0.993, I \text{ in } \mu A, \nu \text{ in mV s}^{-1}) \quad (2)$$

Additionally, the linear relationship between the peak potential (E_{pa}) and ln(ν), which demonstrated in Fig. 7, were investigated and expressed by the equation as below:

$$E_{pa} = 0.0361 \ln(\nu) + 0.990 \; (r^2 = 0.998, E_p \text{ in V}, \nu \text{ in V s}^{-1}) \quad (3)$$

On the other hand, the value of the electron transfer coefficient (α) was calculated using Eq. (5) as follows:

$$E_{pa} = E^{0/} + m \left[0.78 + \ln\left(D^{1/2} k_s^{-1}\right) - 0.5 \ln m \right] + (m/2) \ln(\nu) \quad (4)$$

E_{pa}, $E^{0/}$, ν, and k_s denote the oxidation peak potential, formal potential, potential scan rate, and the electron transfer rate constant, respectively. By plotting the peak potential (E_{pa} in V) versus ln(ν in V s^{-1}), a straight line is obtained with the slope expressed as below:

$$m = RT/[(1-\alpha)n_\alpha F] \quad (5)$$

According to the Eq. (4), the value of m is 0.0722. Consequently, the value of the electron transfer coefficient (α) found to be 0.644 for the irreversible electrode process.

Alternatively, the value of the electron transfer coefficient (α) obtained from the Tafel plot as acquired from the raising part of the current-voltage curve (Fig. 8). The relationship between the log(I) and the peak potential (E_{pa}) was expressed by the following equation:

$$E_{pa} = 0.1576 \log(I) + 0.5187 \; (r^2 = 0.999, E_p \text{ in V}, I \text{ in } \mu A) \quad (6)$$

relationship between the pH and the oxidation peak potential (E_{pa}) which expressed by the equation below with the Nernstian slope of (0.0591x/n), where x and n denote the number of involved hydrogen and the number of electrons transferred throughout the electro-oxidation process, revealed that the number of x and n is equal (see Scheme 1).

$$E_{pa} (V) = -0.0587 \, pH + 1.2458 \; (R^2 = 0.9963) \quad (1)$$

Moreover, the relationship between the potential scan rate and current through the electro-oxidation process of KA was investigated. The obtained cyclic voltammograms revealed that along with an increase in applied scan rates, the peak current was enhanced and shifted to the more positive potentials due to higher overvoltage (see Fig. 6 inset).

According to the following equation which describes the relationship between the square root of scan rate ($\nu^{1/2}$) and the anodic peak currents (I_p), it concluded that the observed irreversible oxidation behavior of KA at the surface of the NiO/

Fig. 6 Plot of I_{pa} versus $\nu^{1/2}$ for the oxidation of KA at NiO/NPs/1B3MITFB/MCPE. Inset shows cyclic voltammograms of 500 μM KA at NiO/NPs/1B3MITFB/MCPE at different scan rates of a 20, b 40, c 80, d 100, e 140, and f 180 mV s^{-1} in 0.1 M phosphate buffer, pH 6.0

y = 8.488X + 10.174
R^2 = 0.993
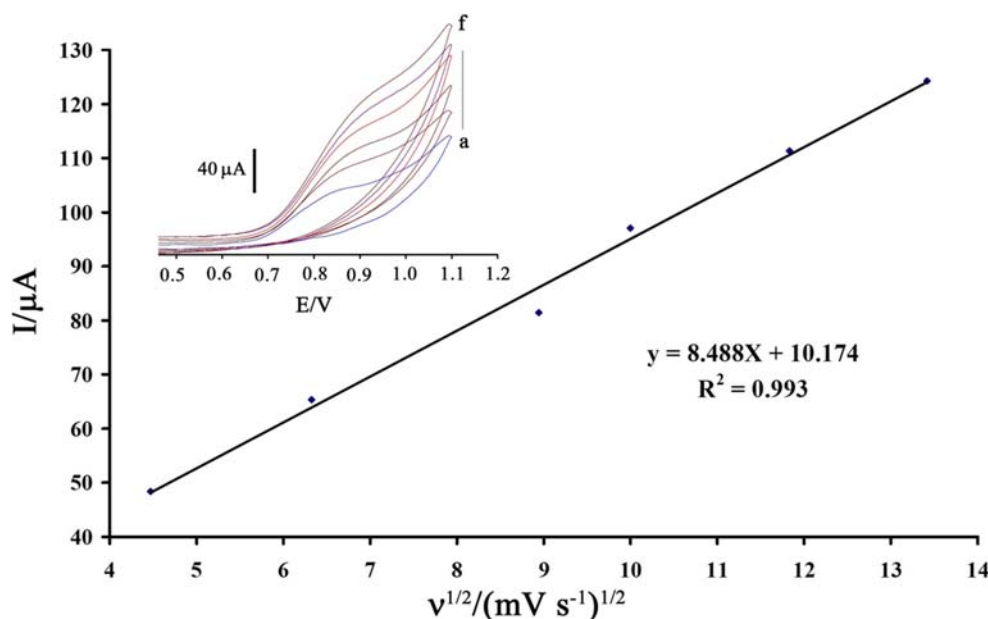
Fig. 7 Plot of potential, E_p, vs. Ln ν for the electro-oxidation of 500 μM KA at a surface of NiO/NPs/1B3MITFB/MCPE at different scan rates of 0.02, 0.04, 0.08, 0.10, 0.14, and 0.18 V s^{-1} in 0.1 M phosphate buffer, pH 6.0
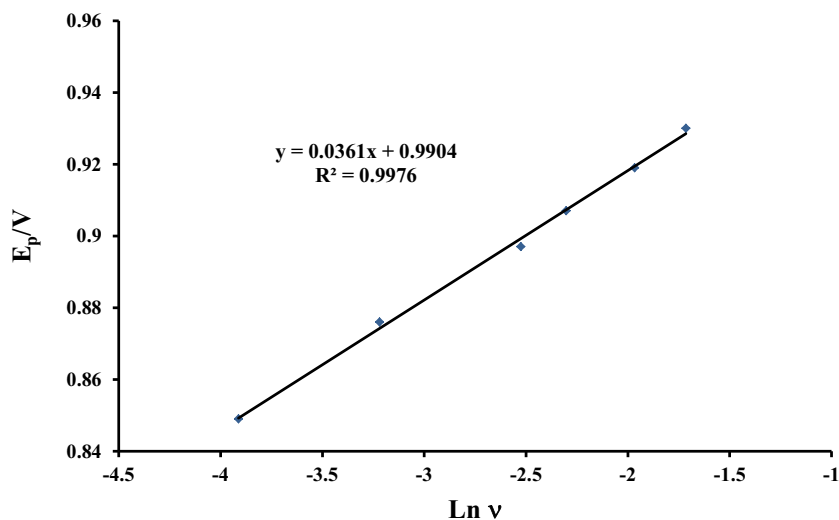
By plotting the peak potential (E_{pa}) versus log(I), a straight line is obtained with the slope expressed as below:
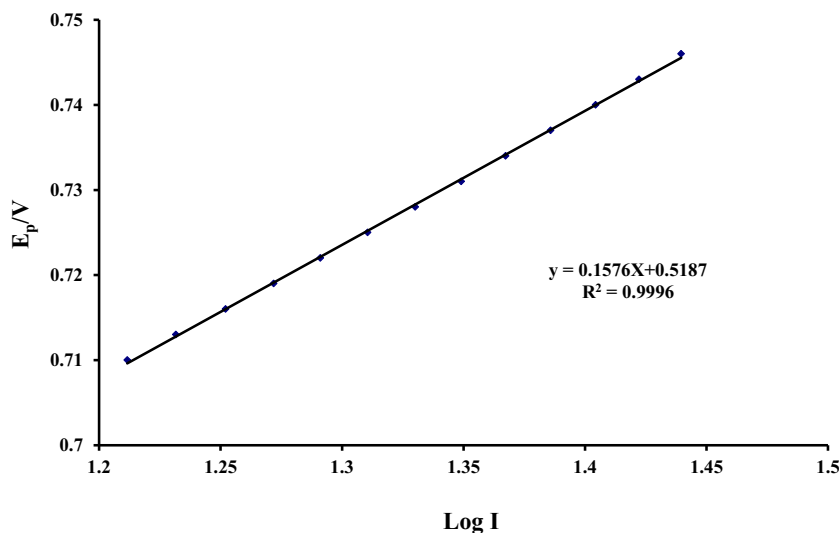
$$m = 2.303\,RT/[(1-\alpha)n_\alpha F] \quad (7)$$

According to Eq. (7), the slope of the Tafel plot comes up to be 0.1576 V decade^{-1}. The amount of calculated α found to be 0.625, which is in the satisfactory agreement with the obtained electron transfer coefficient (α) mentioned above.

3.4 Chronoamperometric Investigation

To evaluate the diffusion coefficient of the KA electro-oxidation process at the mass transport limited rate on the surface of NiO/NPs/1B3MITFB/MCPE, chronoamperometric measurements were carried out [18, 19]. The applied potential was set at 1000 mV vs. Ag/AgCl/KCl$_{sat}$ for the 500 μM and 700 μM of KA in phosphate buffer solutions (pH 6.0)

(Fig. 9a). To calculate the value of the diffusion coefficient (D), the Cottrell equation was employed as follows:

$$I = nFAD^{1/2}\,C/\pi^{1/2}\,t^{1/2} \quad (8)$$

The relationship between the electro-oxidation currents (I) and ($t^{-1/2}$) for different concentrations of KA was demonstrated in Fig. 9b which revealed straight lines with different slopes. By calculating the average value for the diffusion coefficient, the amount of D found to be 2.3×10^{-4} cm^2 s^{-1}.

3.5 Characterization of Fabricated MCPE

The diagnostic performance of the proposed modified sensor with different aspects was examined. For the quantitative determination of KA concentration, the square wave voltammetry technique was employed under the optimum condition. As

Fig. 8 The Plot of potential, E_p, vs. log I for the electro-oxidation of 500 μM KA at a surface of NiO/NPs/1B3MITFB/MCPE at the scan rate of 40 mV s^{-1} in 0.1 M phosphate buffer, pH 6.0

Fig. 9 **a** Chronoamperograms obtained at NiO/NPs/1B3MITFB/MCPE in the presence of **a** 500 and **b** 700 μM KA in the buffer solution (pH 6.0). **b** Cottrell's plot for the data from the chronoamperograms ($n = 1$)
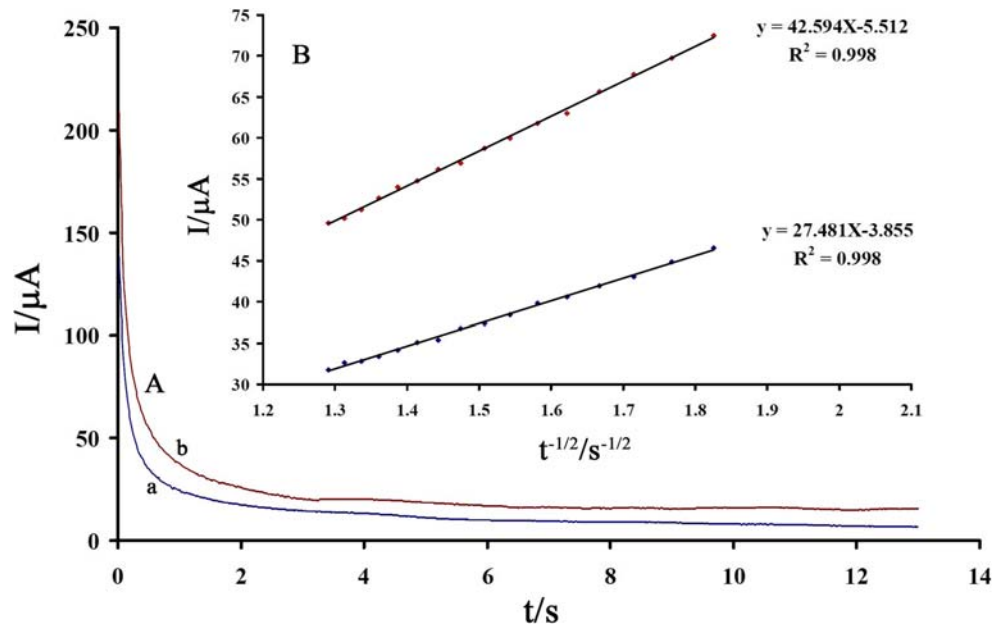
seen from Fig. 10, the obtained calibration curve revealed an adequate linear response over the KA concentration range from 5.0 to 600 μM with the linear regression equation expressed below:

$$I_p \, (\mu A) = (0.0708 \pm 0.0019) \, C_{KA} \tag{9}$$
$$-(0.0346 \pm 0.0052) \, (R^2 = 0.9981, n = 10)$$

The lower detection limit of the proposed sensor found to be 0.8 μM. Table 1 summarized some other relevant reported sensors for the quantitative determination of KA concentration. It is concluded that the developed sensor in the current work revealed a comparable or even better performance. It is

noteworthy to mention that the fabricated NiO/NPs/1B3MITFB/MCPE has some advantages such as easy preparation and low cost compared with other electrodes used in reported works for determination of KA [1, 2, 20].

The long-term stability of the proposed sensor examined after the NiO/NPs/1B3MITFB/MCPE stored for 6 weeks at 25 °C. The obtained results revealed that a negligible drift in peak current observed with a relative standard deviation of 1.3% for the concentration of 10.0 μM KA, which confirmed the satisfactory stability of the developed sensor.

Moreover, to evaluate the reproducibility of the proposed sensor, ten successive measurements of KA concentration were conducted using a standard solution of 10.0 μM KA.

Fig. 10 Plot of peak current as a function of KA concentration. Inset shows the SWVs of NiO/NPs/1B3MITFB/MCPE in 0.1 mol L^{-1} phosphate buffer solution (pH 6.0) correspond to different concentrations of KA including 5, 10, 15, 20, 35, 50, 100, 120, 150, 250, 350, 450, 500, and 600 μM
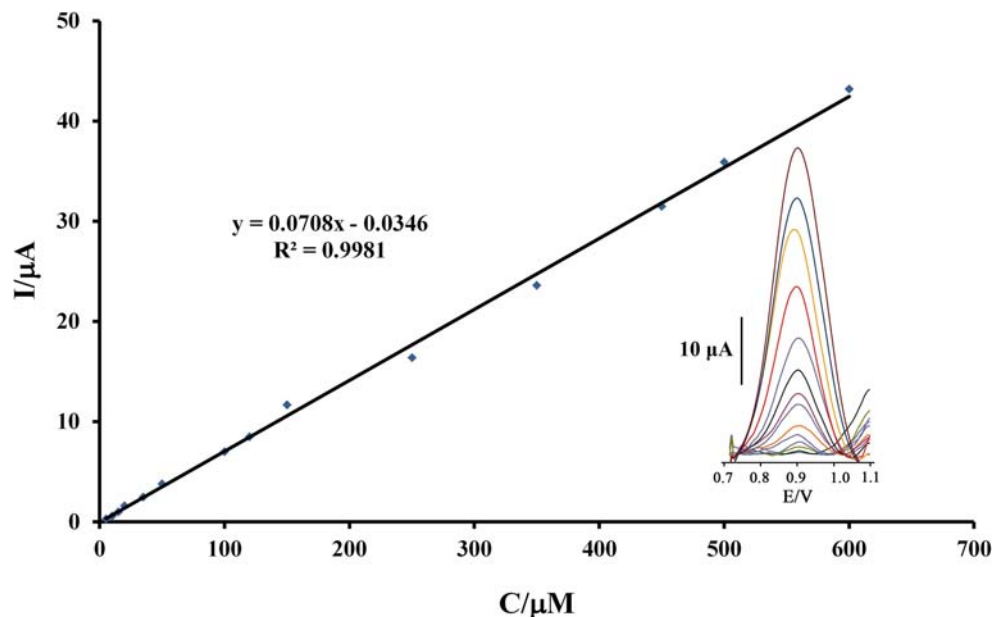
Table 1   Comparison of the efficiency of some modified electrodes used in the voltammetric determination of KA

Electrode	Modifier	Method	pH	LOD (μmol L^{-1})	LDR (μmol L^{-1})	Sensitivity (μA/μmol L^{-1})	Ref.
Glassy carbon	Graphene-Pt nanocomposite	Differential pulse voltammetry	6.0	0.2	0.2–1700	0.003	[1]
Glassy carbon	Molecularly imprinted polymer	Differential pulse voltammetry	5.2	0.003	0.01–0.2	7.6481	[2]
Edge plane pyrolytic graphite	Graphene	Linear sweep voltammetry	6.0	0.23	0.75–15	Not reported	[20]
Carbon paste	NiO/NPs/1B3MITFB	Cyclic voltammetry	6.0	0.8	5.0–600	0.0031	This work

The obtained results revealed good reproducibility of the proposed sensor with a relative standard deviation of 2.4%. On the other hand, the response of the proposed sensor was investigated by immersing it in an aqueous media. The obtained results indicated that the developed electrode revealed stable response within 2.0 h, and afterwards, the background current increased. Moreover, an increase in the background current probably related to partial leakage of 1-butyl-3-methylimidazolium tetrafluoroborate from NiO/NPs/1B3MITFB/MCPE, which resulted in increasing the roughness of the proposed electrode. The proposed sensor revealed a satisfying reproducibility and stability over an adequately long time.

The selectivity of the proposed sensor towards KA was investigated in the presence of some routine potential interference such as glucose, urea, thiourea, amino acids, and electrolyte which exist in blood serum, under the optimum condition. The toleration limit was verified as the highest concentration of the interfering material that made an error of less than ± 5% for the determination of KA. The proposed sensor revealed a successful performance in the term of selectivity, as demonstrated in Table 2.

3.6 Real Sample Analysis

The standard addition method was employed to investigate the applicability of the proposed sensor in the quantitative determination of KA concentration in real samples such as urine, serum, and vinegar (see Table 3).

Moreover, the loading efficiency of KA encapsulation into the liposomes with different chemical compositions evaluated indirectly by the proposed sensor using the supernatant phase.

Table 2   Interference study for the determination of 50.0 μM KA under the optimized condition

Species	Tolerance limits (W/W)
Glucose, urea, thiourea	150
Histidine, methionine, cysteine, lysine, phenyl alanine, glycine	75
Na$^+$, K$^+$, SO$_4^{2-}$, Mg^{2+}, Ca^{2+}, NO$_3^-$, CO$_3^{2-}$, and HCO$_3^-$	100

The obtained results revealed that the liposomal composition of 70:30 (lecithin: cholesterol) demonstrated the highest encapsulation efficiency of 91.0%.

4 Conclusions

A novel high sensitive voltammetric sensor was developed for the quantitative determination of KA concentration in real samples, namely NiO/NPs/1B3MITFB/MCPE. The developed sensor demonstrated superior electrocatalytic activity towards KA in the concentration range of 5.0–600 μM with a lower detection limit of 0.8 μM in aqueous solutions. The conductivity and electron transfer kinetics of the bare and modified electrodes were investigated by electrochemical impedance spectroscopy studies. According to the obtained results, it is concluded that the presence of NiO NPS and 1B3MITFB as a conductive binder significantly increased the KA electro-oxidation process. The acquired data from SEM, XRD, and EDAX analysis confirmed the successful synthesis of NiO nanoparticles with an average diameter of about 20.8 nm using the Scherrer equation. The obtained results revealed that the observed irreversible oxidation behavior of KA at the surface of the NiO/NPs/1B3MITFB/MCPE controlled under the diffusion step with the diffusion coefficient and electron transfer coefficient of 2.3×10^{-4} cm^2 s^{-1} and 0.625, respectively. The proposed sensor was applied successfully for the analysis of trace amounts of KA in

Table 3   Determination of kojic acid in real samples

Samples	Added value (mg mL^{-1})	Expected value (mg mL^{-1})	Founded value (mg mL^{-1})[a]	Recovery (%)
Vinegar	---	---	< Limit of detection	
	10.0	10.0	10.32 ± 0.14	103.20
Urine	---	---	< Limit of detection	
	15.0	15.0	15.72 ± 0.43	104.80
Serum	---	---	< Limit of detection	
	20.0	20.0	20.49 ± 0.22	102.45

[a] Average and standard deviation for triplet measurements

pharmaceutical, biological, and food samples such as liposomal carriers containing KA, human urine and blood serum, and vinegar, respectively.

Compliance with Ethical Standards

Conflict of Interest The authors declare that they have no conflict of interests.

Research Involving Humans and Animals Statement None

Informed Consent None

References

1. Wang, L., Qi, W., Su, R., & He, Z. (2014). Sensitive and efficient electrochemical determination of kojic acid in foodstuffs based on graphene-Pt nanocomposite-modified electrode. *Food Analytical Methods, 7*(1), 109–115.

2. Wang, Y., Tang, J., Luo, X., Hu, X., Yang, C., & Xu, Q. (2011). Development of a sensitive and selective kojic acid sensor based on molecularly imprinted polymer modified electrode in the lab-on-valve system. *Talanta, 85*(5), 2522–2527.

3. Nohynek, G. J., Kirkland, D., Marzin, D., Toutain, H., Leclerc-Ribaud, C., & Jinnai, H. (2004). An assessment of the genotoxicity and human health risk of topical use of kojic acid [5-hydroxy-2-(hydroxymethyl)-4H-pyran-4-one]. *Food and Chemical Toxicology, 42*(1), 93–105.

4. Shih, Y. (2001). Simultaneous determination of magnesium L-ascorbyl-2-phosphate and kojic acid in cosmetic bleaching products by using a microbore column and ion-pair liquid chromatography. *Journal of AOAC International, 84*(4), 1045–1049.

5. Huang, S.-C., Lin, C.-C., Huang, M.-C., & Wen, K.-C. (2004). Simultaneous determination of magnesium ascorbyl phosphate, ascorbyl glucoside, kojic acid, arbutin and hydroquinone in skin whitening cosmetics by HPLC. *Journal of Food and Drug Analysis, 12*(1).

6. Song, P., Xiang, Y., Xing, H., Zhou, Z., Tong, A., & Lu, Y. (2012). Label-free catalytic and molecular beacon containing an abasic site for sensitive fluorescent detection of small inorganic and organic molecules. *Analytical Chemistry, 84*(6), 2916–2922.

7. Yang, Z., Yin, Z., & Chen, F. (2011). A novel kojic acid amperometric sensor based on hollow CuO/Fe 2 O 3 hybrid microspheres immobilized in chitosan matrix. *Electrochimica Acta, 56*(3), 1089–1093.

8. Yang, X., & Zhang, H. (2007). Sensitive determination of kojic acid in foodstuffs using PVP (polyvinylpyrrolidone) modified acetylene black paste electrode. *Food Chemistry, 102*(4), 1223–1227.

9. Mohan, S., Singh, Y., Verma, D. K., & Hasan, S. H. (2015). Synthesis of CuO nanoparticles through green route using Citrus limon juice and its application as nanosorbent for Cr(VI)

remediation: Process optimization with RSM and ANN-GA based model. *Process Safety and Environmental Protection, 96*, 156–166. https://doi.org/10.1016/j.psep.2015.05.005.

10. Ranjbar, M., Ali Taher, M., & Sam, A. (2015). NiO nanostructures: Novel solvent-less solid-state synthesis, characterization and MB photocatalytic degradation. *Journal of Materials Science: Materials in Electronics, 26*(10), 8029–8034. https://doi.org/10.1007/s10854-015-3458-5.

11. Asadollahzadeh, H., Ranjbar, M., & Taher, M. A. (2014). Synthesis and characterization of In2S3 nanostructures via ultrasonic method in the presence of thioglycolic acid. *Journal of Industrial and Engineering Chemistry, 20*(6), 4321–4326. https://doi.org/10.1016/j.jiec.2014.01.039.

12. Ahmadzadeh, S., Karimi, F., Atar, N., Sartori, E. R., Faghih-Mirzaei, E., & Afsharmanesh, E. (2017). Synthesis of CdO nanoparticles using direct chemical precipitation method: Fabrication of novel voltammetric sensor for square wave voltammetry determination of chlorpromazine in pharmaceutical samples. *Inorganic and Nano-Metal Chemistry, 47*(3), 347–353.

13. Zaviska, F., Drogui, P., Blais, J.-F., Mercier, G., & Lafrance, P. (2011). Experimental design methodology applied to electrochemical oxidation of the herbicide atrazine using Ti/IrO 2 and Ti/SnO 2 circular anode electrodes. *Journal of Hazardous Materials, 185*(2), 1499–1507.

14. Salavati-Niasari, M., Ranjbar, M., & Mohandes, F. (2012). Self-assembly of cubic-like nanostructures to form star-like lead sulfate microstructures. *Micro and Nano Letters, 7*(6), 581–584. https://doi.org/10.1049/mnl.2012.0290.

15. Vatanparast, M., Ranjbar, M., Ramezani, M., Hosseinpour-Mashkani, S. M., & Mousavi-Kamazani, M. (2014). Sonochemical approach for synthesis and characterization of PbTe nanostructure. *Superlattices and Microstructures, 65*, 365–374. https://doi.org/10.1016/j.spmi.2013.10.042.

16. Ahmadzadeh, S., & Dolatabadi, M. (2018). Removal of acetaminophen from hospital wastewater using electro-Fenton process. *Environmental Earth Sciences, 77*(2), 53. https://doi.org/10.1007/s12665-017-7203-7.

17. Dolatabadi, M., Mehrabpour, M., Esfandyari, M., Alidadi, H., & Davoudi, M. (2018). Modeling of simultaneous adsorption of dye and metal ion by sawdust from aqueous solution using of ANN and ANFIS. *Chemometrics and Intelligent Laboratory Systems, 181*, 72–78. https://doi.org/10.1016/j.chemolab.2018.07.012.

18. Ahmadzadeh, S., Kassim, A., Rezayi, M., Abdollahi, Y., & Rounaghi, G. H. (2011). A conductometric study of complexation reaction between meso-octamethylcalix[4]pyrrole with titanium cation in acetonitrile-ethanol binary mixtures. *International Journal of Electrochemical Science, 6*(10), 4749–4759.

19. Rezayi, M., Kassim, A., Ahmadzadeh, S., Naji, A., & Ahangar, H. (2011). Conductometric determination of formation constants of tris (2-pyridyl) methylamine and titanium (III) in water-acetonitryl mixture. *International Journal of Electrochemical Science, 6*, 4378–4387.

20. Figueiredo-Filho, L. C., Brownson, D. A., Fatibello-Filho, O., & Banks, C. E. (2013). Exploring the origins of the apparent "electrocatalytic" oxidation of kojic acid at graphene modified electrodes. *Analyst, 138*(16), 4436–4442.